



OPEN

Optimizing speed change lane lengths for two-way ten-lane expressways: a VISSIM and SSAM simulation-based approach

Dan Xiong¹, Quan Yu² & Huihui Guo²✉

With rapid economic development, expressway traffic volumes have surged, resulting in severe congestion. To address this, expanding expressways to two-way ten-lane configurations has become a primary strategy for alleviating traffic pressure. Given the absence of unified national design standards for such highways, this study employs VISSIM microscopic traffic simulation integrated with the Surrogate Safety Assessment Model (SSAM) to investigate the relationship between speed change lane geometries and their design parameters. We evaluate the impacts of varying speed change lane lengths on traffic efficiency and safety under multiple traffic flow conditions for renovated two-way ten-lane expressways. Performance metrics include average delay time, average queue length, conflict frequency, and Post-Encroachment Time (PET). Results demonstrate that at a mainline design speed of 120 km/h, a 270-m acceleration lane reduces traffic conflicts by 47.6% compared to the conventional 230-m benchmark, while a 161-m deceleration lane achieves a 32.8% reduction. This research provides actionable design recommendations for optimizing speed change lane lengths on two-way ten-lane expressways, ultimately enhancing road capacity, safety, and traffic resource allocation efficiency.

Keywords Two-way ten-lane expressway, Speed change lane, SSAM

In recent years, rapid economic growth has significantly increased transportation demand, exceeding the capacity of existing four- to six-lane expressways. Expanding highways to two-way ten-lane configurations has become a primary strategy to alleviate congestion. However, the deployment of ten-lane expressways has exposed nonlinear scaling challenges absent in traditional six-lane standards.

The AASHTO Green Book (2018) specifies a minimum acceleration lane length of 335 m (including tapers) for 100 km/h design speed¹, derived from six-lane scenarios. Critically, this standard fails to address two key ten-lane complexities:

1. Amplified lateral friction effects from extended vehicle paths across five or more lanes;
2. Conflict cascading risks where local disruptions propagate across multiple lanes.

European practices reveal similar gaps. While German RAL Guidelines (2019)² optimize six-lane dynamics, they lack geometric parameters for ten-lane designs such as sight distance adjustments and heavy-truck acceleration zones. Eurocode 1³ defines loads for up to eight lanes but omits ten-lane provisions—treating them as extrapolations rather than distinct systems.

Interchanges remain critical bottlenecks, with ramp terminals accounting for 44–52% of entry/exit crashes⁴. Poor speed change lane designs exacerbate ten-lane-specific risks including extended decision zones in multi-lane merges and speed differentials between inner high-speed lanes and outer truck-dominated lanes.

Although prior studies optimized speed change lanes for six or fewer lanes³, no research has systematically calibrated designs for two-way ten-lane expressways under heavy-truck conditions using integrated VISSIM and SSAM simulation.

Objective and novelty This study bridges this gap by developing a simulation framework to quantify how speed change lane lengths impact traffic efficiency (delay, queue length) and safety (conflict frequency, PET) on ten-lane expressways. Our novel contribution lies in establishing the first evidence-based design calibration for such highways under mixed heavy-truck flows using coupled microsimulation and surrogate safety modeling.

¹Guangdong Transportation Group Co., Ltd, Guangzhou 510000, China. ²North China University of Technology, Beijing 100000, China. ✉email: hueejua@outlook.com

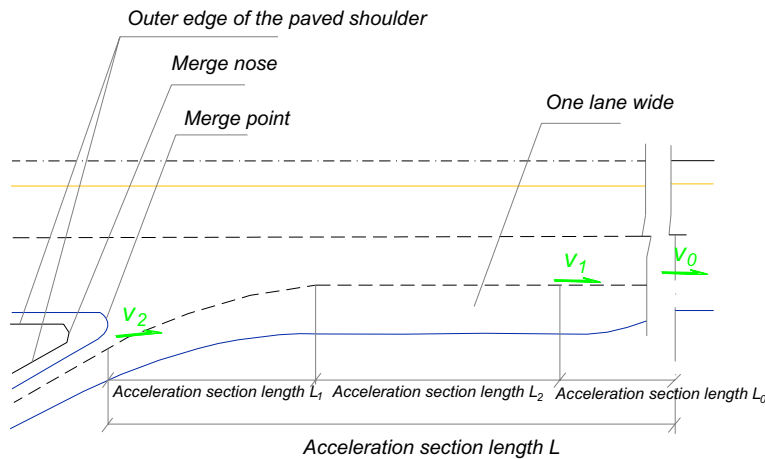


Fig. 1. Parallel Acceleration Lane.

Mainline design speed (km/h)	120	100	80	60
Recommended length of the transition section (m)	90	80	60	50

Table 1. Length of speed change lane transition section. The length of the acceleration section, L_0 , is calculated based on the merging speed V_1 on the mainline and the ramp speed V_2 ⁷:

Interchanges, especially ramp entry and exit points, are major accident hotspots. Reports show that 44% of ramp exit crashes occur at terminal ends, while 52% of ramp entry crashes happen within merging zones⁴. Poorly designed speed change lanes can worsen congestion and safety risks, particularly on multi-lane expressways. While prior studies have explored conventional speed change lane designs, research on high-capacity, ten-lane expressways remains limited.

The reconstructed GuangShao Expressway is a two-way ten-lane expressway with multiple lanes, a wide cross-section, and complex traffic organization⁵. This study employs VISSIM simulation and the Surrogate Safety Assessment Model (SSAM) to systematically evaluate the effects of varying speed change lane lengths on traffic efficiency and safety under different traffic flow conditions. The objective is to provide scientific guidance for designing speed change lanes on two-way ten-lane expressways, enhancing road performance, meeting transportation demands, and improving national expressway safety and efficiency.

Calculation of speed change lane length

Given the high proportion of heavy-duty trucks on expressways in China and their limited acceleration capabilities, ensuring sufficient space for safe merging without queuing or forced merging is crucial to prevent safety risks. Longer parallel acceleration lanes are therefore necessary. In contrast, the design of deceleration lanes should prioritize both driver convenience and safety. Since parallel deceleration lanes often involve complex trajectories, direct deceleration lanes are commonly employed⁶. The calculations in this study are based on the design of parallel acceleration and direct deceleration lanes.

Calculation of acceleration lane length

Vehicles accelerate along the parallel acceleration lane segment, designated as L_1 , until they reach the mainline speed, V_1 . They then wait in the auxiliary section, designated as L_2 , until a suitable gap appears in the outer lane of the mainline, at which point they merge. This process is illustrated in Fig. 1.

The total length of the acceleration lane is calculated as follows:

$$L_{\text{acc}} = L_0 + L_1 + L_2 \quad (1)$$

where L_0 , L_1 , and L_2 represent the lengths of the transition section, acceleration section, and auxiliary (waiting) section, respectively. The value of L_0 is derived from Table 1.

$$L_1 = \frac{V_1^2 - V_2^2}{25.92a} \quad (2)$$

Here, a represents the average acceleration in the L_1 segment, which is set at 1.2 m/s^2 in accordance with the Highway Route Design Specifications (JTG D20-2017). The initial speed V_a on the mainline is equivalent to V_1 , while the ramp's design speed is represented by V_2 .

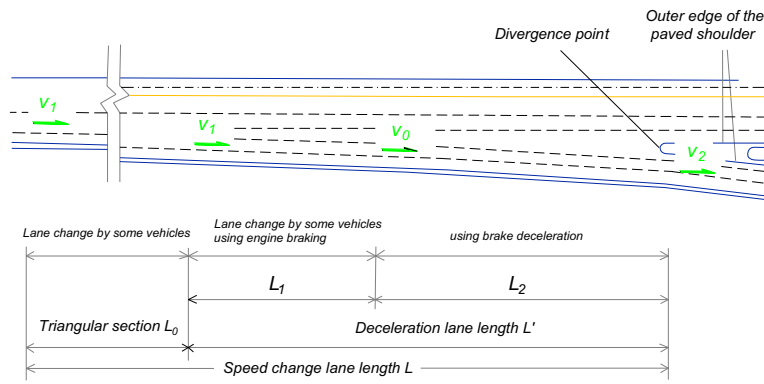


Fig. 2. Direct deceleration lane.

Mainline design speed (km/h)	80	100	120
30	124	150	175
40	116	143	168
50	107	135	161
60	97	126	153
70	73	104	134
80	–	–	97

Table 2. Length of direct deceleration lane.

The auxiliary lane length, L_2 , is the distance traveled by vehicles while searching for a suitable merging gap. It is calculated as follows:

$$L_2 = \frac{v_1 t_w}{3.6} \quad (3)$$

where t_w is the average waiting time for vehicles to find a merging gap. Based on the calculations in Eq. (1) to (3), the lengths of parallel acceleration lanes for different design speeds were determined. The resulting data is shown in Table 2.

Calculation of deceleration lane length

In the direct deceleration lane, vehicles first pass through the transition section, L_0 , at speed V_0 . In segment L_1 , the vehicle decelerates using engine braking for three seconds to reach speed V_1 . In segment L_2 , the vehicle continues to decelerate to the ramp's average speed, V_2 , with both deceleration rates remaining constant throughout each segment, as shown in Fig. 2.

Therefore, the formula for calculating the deceleration lane length is given by⁷:

$$L_{\text{dec}} = L_0 + L_1 + L_2 \quad (4)$$

where L_0 is the length of the transition section (refer to the recommended values in Table 1), L_1 is the length of the engine braking deceleration section, and L_2 is the length of the braking deceleration Sect.

$$L_1 = \frac{V_0 t_d}{3.6} = \frac{a_1 t_d^2}{2} \quad (5)$$

$$L_2 = \frac{V_1^2 - V_2^2}{25.92 a_2} = \frac{(V_0 - 3 \cdot 6 a_1 t_d)^2 - V_2^2}{25.92 a_2} \quad (6)$$

In this equation, V_0 represents the average speed of vehicles on the mainline before deceleration, which is equivalent to the initial speed V_a ; t_d is the duration of engine braking, set to 3 s; a_1 represents the engine's deceleration rate, and a_2 represents the deceleration rate of the brake system; V_1 is the speed after engine braking, and V_2 is the average speed of the ramp.

Based on Eq. (4) to (6), the lengths of the direct deceleration lanes on the mainline and ramp for different design speeds are calculated, as shown in Table 2.



Fig. 3. Detector setup and traffic data capture zones for the interchange entrance of G4 Beijing-Hong Kong-Macao expressway and G45 Daqing-Guangzhou expressway.

计数: 168	仿真运行	时间 ...	数据采...	加速度(所...	距离(所有)	长度(所有)	车辆(...	人数(...	速度的算数...	速度的调和...	占有率(所有)
13	4	0-3600	1	0.02	887.27	5.47	952	952	82.32	78.73	41.28%
14	4	0-3600	2	-0.23	504.05	5.59	930	930	85.18	81.12	40.97%
15	4	0-3600	3	0.16	461.12	5.39	257	257	61.43	60.82	17.96%
16	4	0-3600	4	-0.04	678.84	5.67	207	207	68.90	68.30	13.81%
17	5	0-3600	1	0.10	882.11	5.53	1510	1510	70.66	66.85	53.40%
18	5	0-3600	2	-0.79	503.94	5.60	1248	1248	77.46	73.17	44.50%
19	5	0-3600	3	0.03	461.10	5.34	347	347	61.02	60.38	18.38%
20	5	0-3600	4	0.08	674.19	5.48	78	78	60.88	59.38	4.38%

Fig. 4. Traffic operation data recorded at detection points for the interchange entrance simulation.

Analysis of safety impacts based on VISSIM simulation and SSAM

VISSIM, developed by PTV Group, is a microscopic simulation software designed to model urban and public transportation systems based on realistic driving behaviors and time intervals. It simulates various components, including lanes, traffic flows, signals, and public transit, providing an effective tool for evaluating traffic planning schemes⁸.

Simulation of acceleration lanes

A VISSIM simulation was employed to construct a network model accurately representing the merging and diverging traffic flows at highway entrances and exits. The model was based on the existing road conditions, specifically the section where the G4 Beijing-Hong Kong-Macao Expressway intersects with the G45 Daqing-Guangzhou Expressway at a single-direction, five-lane merging point. The length of the simulated acceleration lane, including the auxiliary lane, was set at 230 m. The transition section and lane width were specified as 90 m and 3.75 m, respectively. As illustrated in Fig. 3, detectors were positioned 200 m before and after the entrance to record real-time traffic flow data for each lane in the vicinity of the event-triggering region.

The mainline traffic flow was set at 8000, 9000, and 10,000 vehicles per hour (veh/h), with corresponding ramp traffic flows of 3000, 3300, and 3600 veh/h, respectively. The simulation was conducted with the highest precision, using a time step of one second per simulation second. Each simulation run lasted 3600 s. Based on the traffic composition, the relative proportions of passenger cars and heavy-duty trucks, as well as their desired speeds, were defined. Traffic operation data recorded at the detection points are shown in Fig. 4.

To ensure that our VISSIM model accurately represents real traffic conditions, a rigorous calibration and validation process was carried out. The calibration involved adjusting model parameters such as vehicle arrival rates and driver behavior characteristics to match observed field data. Particular attention was given to key parameters like vehicle desired speeds and following distances, which were calibrated using field observation data collected from the study site. This calibration process involved comparing simulated traffic flow characteristics with real-world traffic data to ensure that the model accurately reflects actual driving behaviors. For validation, simulated traffic speeds and flow rates were compared with actual measurements collected from the study site. The model was fine-tuned until the simulated results closely aligned with the real-world observations, ensuring a high level of confidence in the model's ability to replicate real traffic scenarios. Additionally, the following assumptions were made in the simulation setup: vehicle type distribution was set according to regional traffic statistics, no incidents or breakdowns occurred during the simulation period, and road conditions were maintained in a dry state to avoid the influence of adverse weather on traffic operations.

As specified in the Highway Route Design Specifications (JTG D20-2017), the eight-lane two-way expressway was expanded to a ten-lane configuration. The average delay time and queue length for the 230-meter acceleration

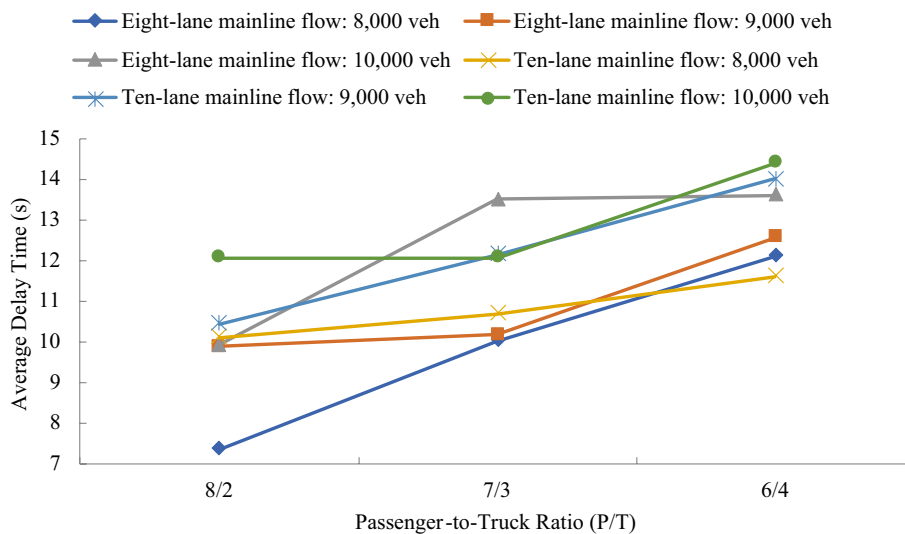


Fig. 5. Comparison of average delay.

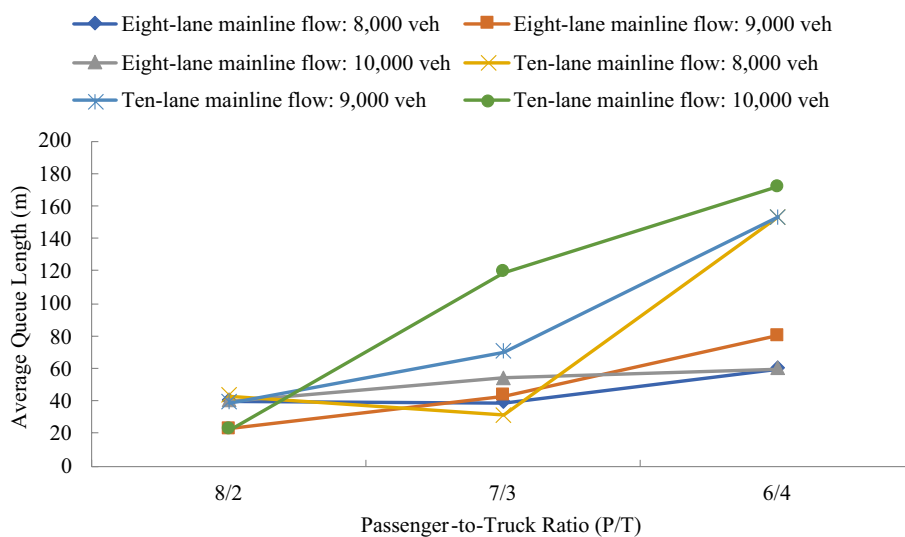


Fig. 6. Comparison of average queue length.

lane after expansion were compared to those of a standard two-way ten-lane expressway. The results are shown in Figs. 5 and 6.

As the number of lanes increases, the rise in mainline traffic flow significantly reduces vehicle speeds, leading to congestion in merging areas. Changes in traffic flow parameters, such as increased mainline input flow and a higher proportion of heavy-duty trucks, exacerbate congestion in the merging area, negatively affecting traffic efficiency. As the proportion of heavy-duty trucks increases, both queue lengths and stop delays rise substantially. The analysis reveals that the conventional 230-m acceleration lane in the merging section of a two-way ten-lane expressway is highly sensitive to traffic flow variations and insufficient to alleviate congestion.

The acceleration lane length data for a mainline design speed of 120 km/h, calculated from Table 2, was analyzed to generate a comparison chart of average delays for different acceleration lane lengths on two-way ten-lane expressways, as shown in Fig. 7.

When mainline traffic flow is low, vehicle spacing is larger, and ramp merging delays are minimal. However, as mainline traffic flow increases, ramp vehicles must wait for suitable gaps in the mainline flow, resulting in greater delays. Additionally, higher proportions of heavy-duty trucks further aggravate traffic delays.

A comparison of queue lengths for different acceleration lane lengths was generated using simulation data, as shown in Fig. 8. The results indicate that the average queue length in the merging area increases with higher mainline traffic flow and a greater proportion of heavy-duty trucks.

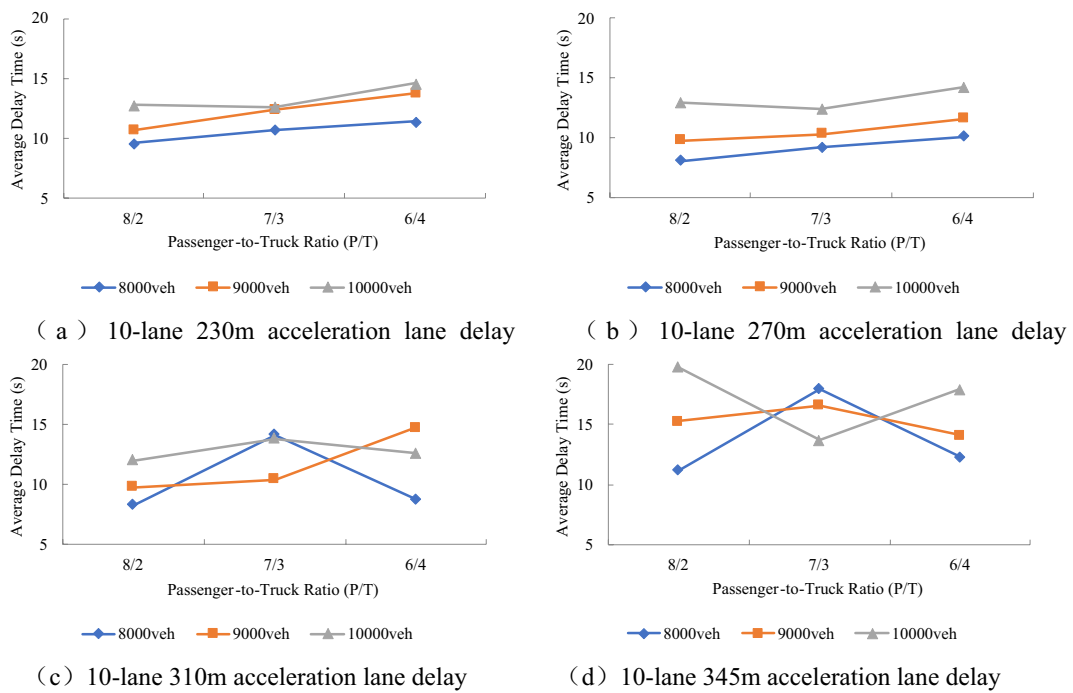


Fig. 7. Comparison of average delay.

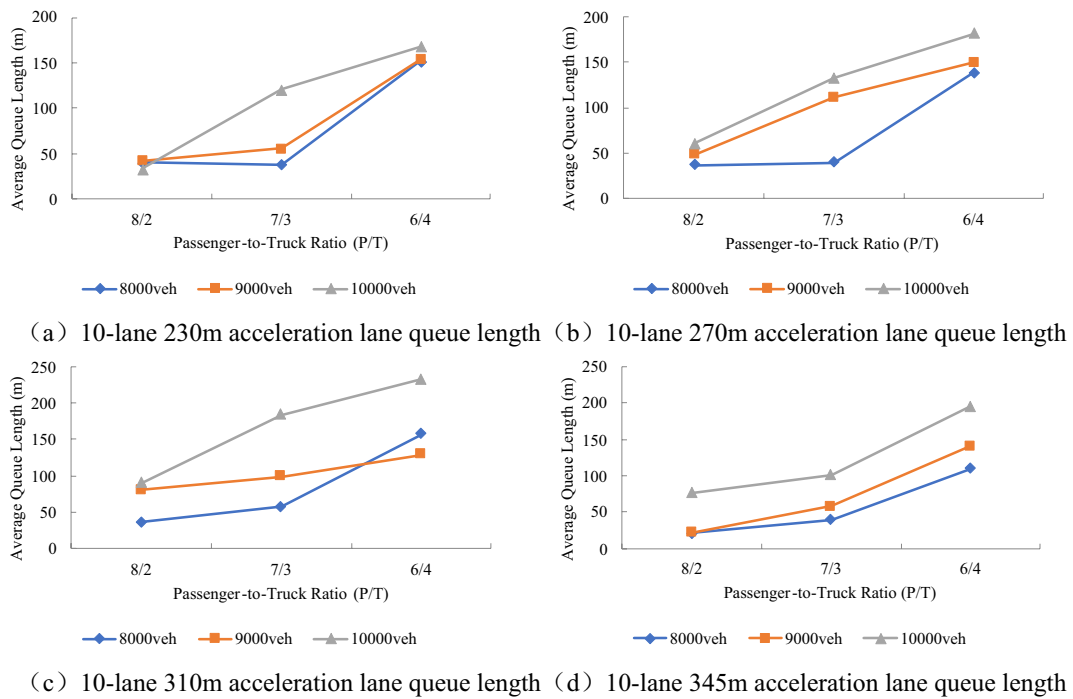


Fig. 8. Comparison of average queue length.

Simulation of deceleration lanes

The road parameters for the deceleration lane were based on the section where the G4 Beijing-Hong Kong-Macao Expressway intersects with the G45 Daqing-Guangzhou Expressway at a single-direction, five-lane merging point. In the simulation, the deceleration lane, including the auxiliary lane, was assigned a length of 145 m. The transition section length and lane width were specified as 100 m and 3.75 m, respectively. Detectors were positioned 200 m upstream and downstream of the entrance to record real-time traffic data for each lane within the event-triggering zone, as shown in Fig. 9.



Fig. 9. Detector setup and traffic data capture zones for the interchange exit of G4 Beijing-Hong Kong-Macao expressway and G45 Daqing-Guangzhou expressway.

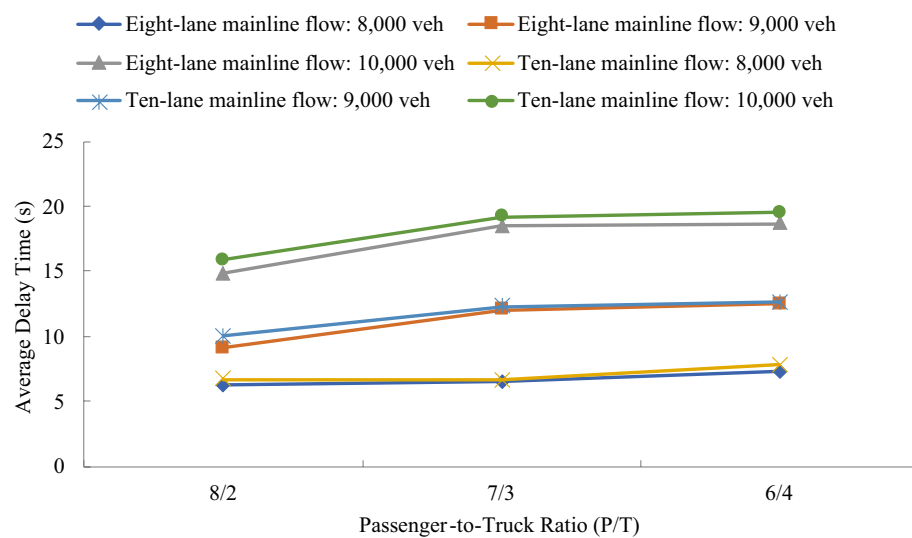


Fig. 10. Comparison of average delay.

The mainline input traffic flow was set at 8000, 9000, and 10,000 vehicles per hour (veh/h). The simulation was conducted with high precision, using a time step of one second per simulation second, and each simulation run lasted 3600 s. Based on the actual traffic composition, the relative proportions of passenger cars and heavy-duty trucks, as well as their desired speeds, were defined in accordance with observed traffic patterns. During the simulation, vehicle detection points within the network recorded real-time raw traffic flow data.

To enhance the reliability of the simulation model for the deceleration lane, the same rigorous calibration and validation approach was applied as in the acceleration lane simulation. Key parameters, including vehicle desired speeds and following distances, were carefully calibrated against field observation data to ensure they align with real-world driving behaviors. The simulation setup also maintained the same assumptions regarding vehicle type distribution, incident-free conditions, and dry road conditions as mentioned in the acceleration lane simulation.

In line with the specifications outlined in the Highway Route Design Specifications (JTG D20-2017), the two-way eight-lane expressway was expanded to a two-way ten-lane configuration with the addition of a 145-m deceleration lane. The average delay time and queue length of the ten-lane expressway were subsequently compared before and after the expansion, particularly following the addition of the deceleration lane, to assess the effectiveness of the upgrade. The results are shown in Figs. 10 and 11.

As the number of lanes increases and mainline traffic flow grows, vehicle speeds decrease significantly, leading to congestion in diverging areas. Adjustments to traffic flow, such as increasing mainline input flow and the proportion of heavy-duty trucks, reduce traffic efficiency in the diverging area. Analysis shows that the traditional 145-m deceleration lane in the diverging section of a two-way ten-lane expressway is highly sensitive to traffic flow variations and insufficient to alleviate congestion.

Statistical analysis of simulation results, based on deceleration lane length data for a mainline speed of 120 km/h from Table 2, was conducted to evaluate vehicle delay times under different deceleration lane lengths, passenger-to-truck ratios, and traffic flows. The findings are presented in Fig. 12, while the corresponding mean queue lengths are shown in Fig. 13. When traffic flow approaches saturation, congestion occurs, vehicles begin to queue, and delays increase. As depicted in Fig. 13, both average delays and queue lengths rise with greater mainline traffic flow and higher proportions of heavy-duty trucks.

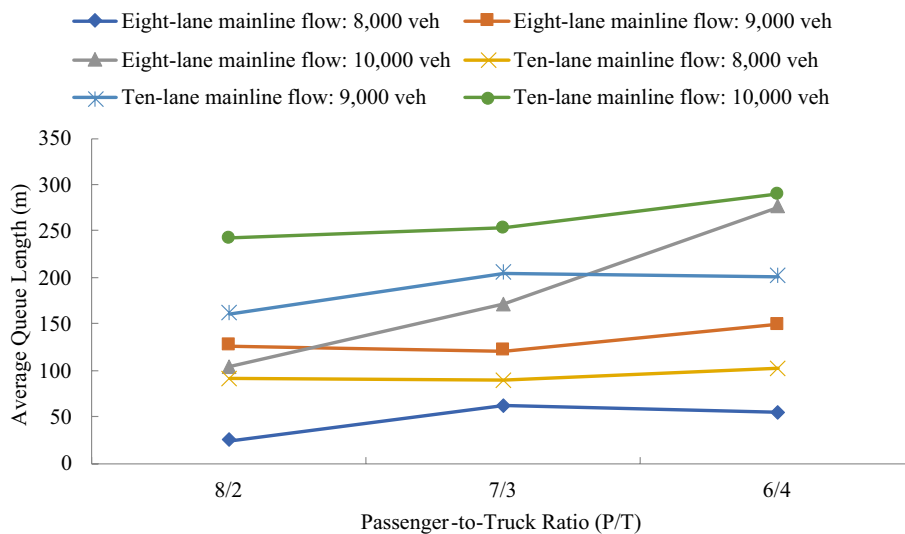


Fig. 11. Comparison of average queue length.

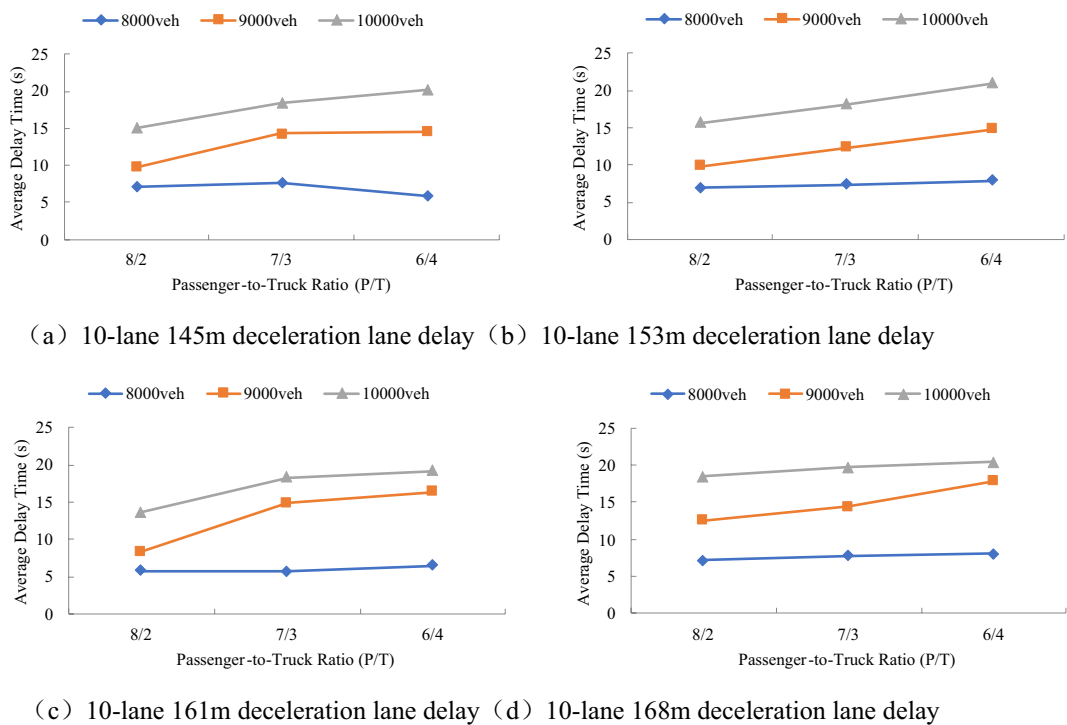


Fig. 12. Comparison of average delay.

As illustrated in Fig. 13, the mean queue length in the diverging area increases with higher mainline traffic flow and a greater proportion of heavy-duty trucks.

Evaluation using SSAM

The conventional approach to traffic safety evaluation relies on comprehensive historical accident data. However, this method is not suitable for projects that lack sufficient statistical data or are still in the planning stages. The Siemens research team proposed the Surrogate Safety Assessment Model (SSAM)⁹, which uses traffic simulation software to construct models. Through algorithms, it analyzes traffic conflicts within the simulation, identifies conflicts from vehicle trajectories, and generates safety evaluation metrics for assessing both existing and planned traffic scenarios^{10–12}.

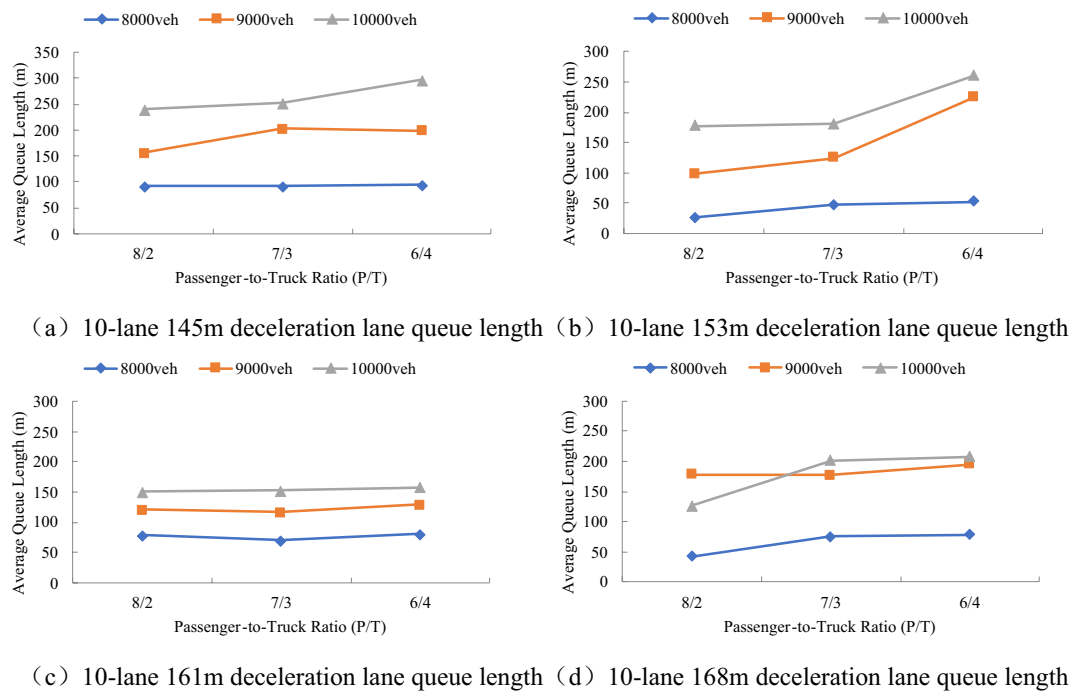


Fig. 13. Comparison of average queue length.

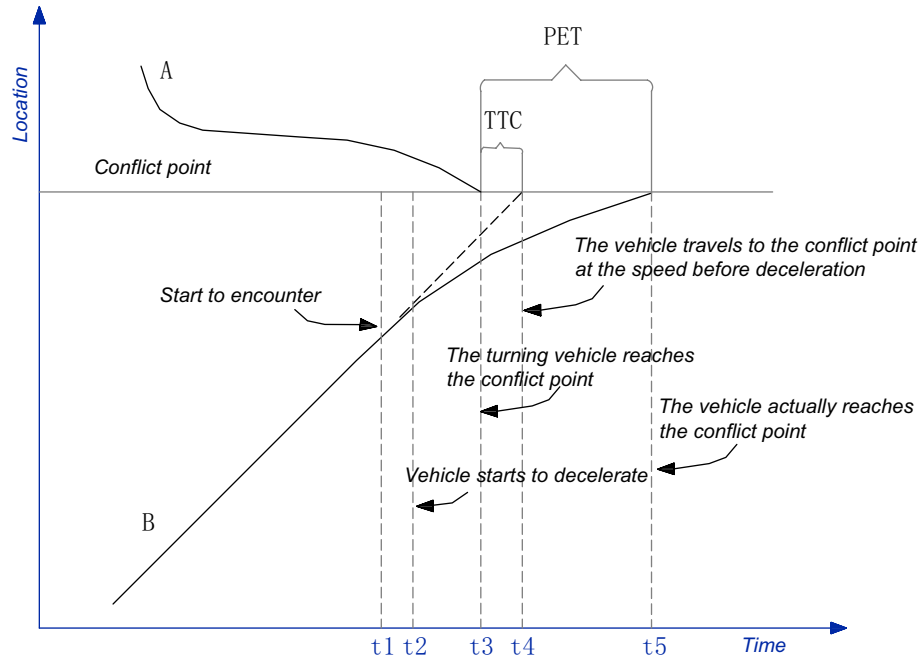


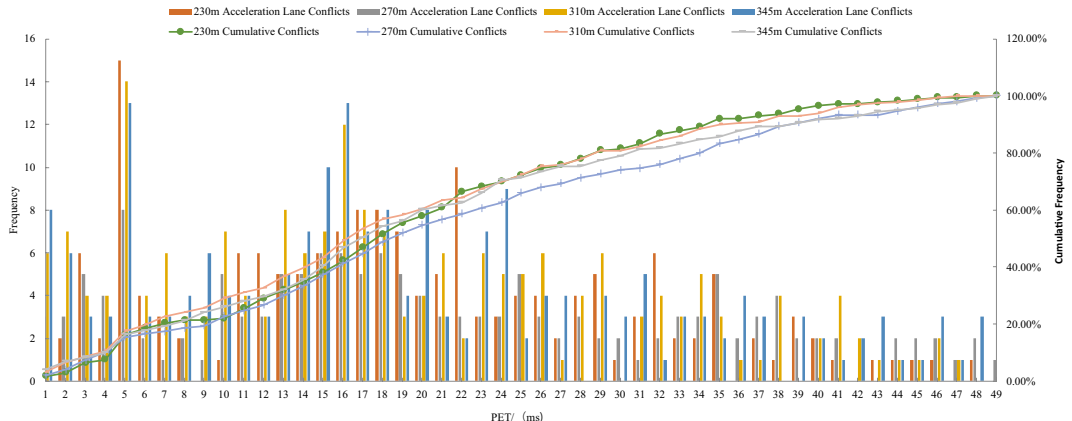
Fig. 14. Time-space trajectory of vehicle conflicts.

The SSAM system provides detailed data on the characteristics of simulated conflicts, including their number, type, severity, and location. Severity is assessed using five indicators: Time to Collision (TTC), Post-Encroachment Time (PET), Deceleration Rate (DR), Maximum Speed (MaxS), and Speed Difference (DeltaS)^{13,14}.

The calculation methods for each conflict indicator are shown in Fig. 14¹⁵. The following definitions apply to the times represented in the figure:

- t1: Vehicle A enters the conflict zone.
- t2: Vehicle B receives a collision warning from Vehicle A and initiates evasive action, beginning to decelerate.
- t3: Vehicle A exits the conflict zone.
- t4: In the absence of evasive action, the predicted time for vehicle B to reach the conflict point.

PET/s	Acceleration lane length (m)			
	230	270	310	340
0.1	3	3	6	8
0.2	2	3	7	6
0.3	6	5	4	3
0.4	2	4	4	3
0.5	15	8	14	13
0.6	4	2	4	3
0.7	3	1	6	3
0.8	2	2	3	4
0.9	0	1	3	6
1.0	1	3	7	4
1.1	6	3	4	4
1.2	6	3	3	3
1.3	5	5	8	5
1.4	5	5	6	7
1.5	6	6	7	10

Table 3. Partial table of conflict PET indicators for different acceleration lanes.**Fig. 15.** Cumulative PET curve of conflicts in the acceleration lane merging area before and after optimization.

t5: The actual time at which vehicle B reaches the conflict point.

VISSIM simulations were performed for the merging area at the entrance of the ten-lane expressway. The SSAM model was used to analyze conflicts in the trajectory data and assess the safety impact of different lane lengths. It should be noted that SSAM, while a powerful tool for safety assessment, has certain limitations. For instance, it assumes standard driver reaction times and does not account for variations in driver behavior such as sudden maneuvers or differences in driver experience. Additionally, SSAM primarily focuses on conflict analysis and may not fully capture all aspects of traffic safety, such as the impact of environmental factors or the effects of traffic control measures. Furthermore, the model relies on simulated data, which may not perfectly represent real-world conditions due to simplifications and assumptions made during the modeling process.

The maximum critical value for PET is set at 5 s, and for a mainline design speed of 120 km/h, the simulation results for conflict numbers at different acceleration lane lengths are shown in Table 3.

A normal curve analysis was conducted on the PET data using SPSS. The distribution of traffic conflicts for the 230-m acceleration lane ranged from -6 to 15, with an average of 3.48. For the 270-m acceleration lane, the conflict count ranged from -4 to 10, with an average of 3.02. For the 310-m acceleration lane, the conflict count ranged from -6 to 15, with an average of 4.12, and for the 345-m acceleration lane, the conflict count ranged from -6 to 15, with an average of 3.98.

The conflict data were categorized into three levels: severe, minor, and potential conflicts. The cumulative frequency distribution is shown in Fig. 15. Based on normal distribution theory, the 15th and 85th percentiles were used to define the thresholds for severe and potential conflicts. The results indicated that the PET threshold for severe conflicts was 0.3 s, while the threshold for potential conflicts was 3.3 s. These thresholds were determined based on a normal distribution analysis of the PET data. Using SPSS, a normal curve analysis was performed, and the 15th and 85th percentiles of the cumulative frequency distribution were used to define

the thresholds for severe and potential conflicts. This approach is consistent with common practices in traffic conflict analysis, where the lower percentile represents severe conflicts that require immediate attention, and the higher percentile represents potential conflicts that may affect traffic safety and flow.

Using the 15th percentile of the cumulative frequency distribution, a critical threshold of approximately 0.3 s was set for severe conflicts. The remaining conflict data were divided into two categories, with the PET value of approximately 3.3 s serving as the boundary between minor and potential conflicts.

According to this threshold-setting method, traffic conflicts in the optimized expressway merging areas were classified into three levels: severe, minor, and potential conflicts. The PET threshold ranges were as follows: $\text{PET} > 3.3$ s for potential conflicts, $0.3 < \text{PET} \leq 3.3$ s for minor conflicts, and $\text{PET} \leq 0.3$ s for severe conflicts.

The analysis indicated that the 270-m acceleration lane consistently exhibited lower conflict PET indices compared to other options, with a 47.6% reduction in traffic conflicts compared to the traditional lane length. This design aligns with the statistically recommended design speed for the current entrance ramp.

Observations show that when vehicles merge from the entrance ramp onto the mainline, they initially decelerate at the end of the ramp to observe the mainline traffic flow and assess whether there is a sufficient gap for merging. When traffic density is high, vehicles tend to continue along the acceleration lane until a suitable and safe gap in the mainline flow is found. The length of the acceleration lane significantly affects the incidence of traffic conflicts. Shortening the acceleration lane in the merging section may prevent vehicles from accelerating adequately, increasing the risk of conflicts between vehicles entering the mainline and those already on the ramp.

A similar analysis was performed for the deceleration lane. When the mainline design speed is 120 km/h and the deceleration lane is 161 m long, the conflict PET index for the exit ramp is lower than for other configurations, showing a 32.8% reduction in traffic conflicts compared to the traditional length. It is recommended that the speed limit for the diverging ramp be set at 40 km/h, consistent with the statistically recommended design speed for the current exit ramp.

This study, based on experimental data at 120 km/h, also accounts for a safety margin for designs at lower speeds, including 100 km/h. The findings are primarily applicable to the traffic composition and driving behaviors observed on Chinese expressways, where the specific mix of vehicle types, traffic flow characteristics, and driver behavior patterns were integral to the simulation scenarios and analysis. While the general trends and design recommendations may offer insights for other regions with similar traffic conditions, their direct applicability to highways in other areas should be carefully evaluated considering local traffic composition, driving behaviors, and regulations. For the GuangShao Expressway reconstruction project, even with a reduction in the mainline design speed to 100 km/h, the proposed optimization strategy can still ensure both safety and efficiency, providing scientific guidance for expressway design under various speed conditions. However, it is important to conduct additional validation and calibration when applying these findings to different traffic environments.

Conclusion

This study utilized VISSIM simulation software to model traffic conditions before and after the implementation of the road optimization design. A set of traffic flow evaluation metrics were then developed using SSAM to assess the effectiveness of the optimization.

When the entrance ramp acceleration lane length was set to 270 m, with a 90-m transition section, the average delay time, average queue length, and occurrence frequency at the entrance were significantly reduced compared to other configurations. Additionally, the number of vehicle conflicts was also markedly lower. Similarly, when the exit ramp deceleration lane length was set to 161 m with a 90-m transition section, the results were outstanding, showing a clear reduction in average queue occurrences, queue lengths, and average stop delays compared to other configurations. The optimized design significantly improved both the traffic efficiency and safety of the two-way ten-lane expressway entrance and exit, while effectively reducing potential conflict points.

This study primarily focused on the driving speed of vehicles at entrance and exit ramps as the basis for analyzing speed change lanes. However, it did not include a sensitivity analysis to examine how variations in traffic conditions, such as changes in traffic flow, vehicle composition, or driver behavior, might affect the results. Future research should incorporate sensitivity analysis and additional evaluation metrics to further assess the robustness of the conclusions and enhance the reliability of the findings.

The contribution of this research lies not only in offering specific design recommendations for the GuangShao Expressway reconstruction project but also in advancing the methodology for evaluating and optimizing speed change lane designs on high-speed roadways. By combining VISSIM simulations with SSAM analysis, this study provides a practical example of how to assess and enhance traffic safety and efficiency in complex highway environments. This approach can serve as a valuable reference for transportation engineers and planners working on similar infrastructure projects.

Data availability

The datasets generated and/or analysed during the current study are not publicly available due to containing sensitive business information of a collaborating third - party company. Unauthorized disclosure may cause harm to the company's interests. but are available from the corresponding author on reasonable request. Interested parties can contact the corresponding author at hueejuoa@outlook.com with a detailed research purpose, and relevant non-disclosure agreements will be signed before data release.

Received: 13 March 2025; Accepted: 30 June 2025

Published online: 26 August 2025

References

1. AASHTO. *A Policy on Geometric Design of Highways and Streets* 7th edn (American Association of State Highway and Transportation Officials, 2018).
2. German Federal Ministry of Transport and Digital Infrastructure. *Guidelines for the Design of Motorways (RAL)* (BMVI, 2019).
3. European Committee for Standardization. *Eurocode 1: Actions on structures – Part 2: Traffic Loads on Bridges* (EN 1991-2) (CEN, 2020).
4. He, X. F., Xiong, W. L. & Li, Z. J. Study on the selection of transverse slope of roadway crown in the design of highway reconstruction and expansion with ultra-wide sections. *Highways Automot. Appl.* **40** (1), 91–94 (2024).
5. Tian, S. M. et al. Analysis of the current characteristics and trends of traffic demand on National expressways. *Mod. Transp. Metall. Mater.* **2** (3), 18–26 (2022).
6. Zhang, C. et al. A review on the safety of highway interchange entrances and exits. *J. Transp. Inform. Saf.* **41** (2), 1–17 (2023).
7. Xu, Q. S. *Research on Safety Design Methods for Highway Interchange Bridges [D]* (Beijing University of Technology, 2008).
8. Xing, X. L. *Study on the Length of Variable Speed Lanes on Expressways [D]* (Xi'an, 2013).
9. Calvi, A., Benedetto, A. & De Blasiis, M. R. A driving simulator study of driver performance on deceleration lanes. *Accid. Anal. Prev.* **45**, 195–203 (2012).
10. Lin, L. P. *Research on Traffic Conflict Prediction and Safety Evaluation in Expressway Merging Areas [D]* (Harbin Institute of Technology, 2017).
11. Cao, H. W. *Research on Regional Traffic Coordination and Optimization Control Based on Vehicle Average Delay Model [D]* (Nanjing University of Posts and Telecommunications, 2020).
12. Zhang, X. H. *Research on Traffic Conflict Prediction and Safety Evaluation in Merging Areas of Expressway Interchanges [D]* (Chang'an University, 2021).
13. Ye, H. B. & Liao, C. F. Traffic safety evaluation of intersections based on SSAM. *Urban Roads Bridges Flood Control.* **3**, 34–40 (2016).
14. Muley, D., Ghannim, M. & Kharbeche, M. Prediction of traffic conflicts at signalized intersections using SSAM. *Procedia Comput. Sci.* **130**, 255–262 (2018).
15. Huang, F. Research on the effectiveness verification of safety evaluation in expressway merging areas based on SSAM. In *Proceedings of the 2018 Annual Conference on Urban Transport Planning in China*, 9. Southeast University Press. (2018).

Author contributions

D.X. and Q. Y. conceptualized the study and designed methodology; H.G. and Q.Y. collected and curated data; D.X. performed formal analysis and validation; H.G. wrote the original draft; D.X. and Q.Y. visualized results and prepared Figs. 1, 2, 3, 4, 5, 6, 7, 8, 9, 10, 11, 12, 13, 14 and 15, D, , D, and D.X. supervised project execution; R.T. secured funding and oversaw resources. All authors (D.X., Q. Y., H.G.) reviewed and edited the manuscript, approved the final version, and agreed to be accountable for the work.

Declarations

Competing interests

The authors declare no competing interests.

Additional information

Correspondence and requests for materials should be addressed to H.G.

Reprints and permissions information is available at www.nature.com/reprints.

Publisher's note Springer Nature remains neutral with regard to jurisdictional claims in published maps and institutional affiliations.

Open Access This article is licensed under a Creative Commons Attribution-NonCommercial-NoDerivatives 4.0 International License, which permits any non-commercial use, sharing, distribution and reproduction in any medium or format, as long as you give appropriate credit to the original author(s) and the source, provide a link to the Creative Commons licence, and indicate if you modified the licensed material. You do not have permission under this licence to share adapted material derived from this article or parts of it. The images or other third party material in this article are included in the article's Creative Commons licence, unless indicated otherwise in a credit line to the material. If material is not included in the article's Creative Commons licence and your intended use is not permitted by statutory regulation or exceeds the permitted use, you will need to obtain permission directly from the copyright holder. To view a copy of this licence, visit <http://creativecommons.org/licenses/by-nc-nd/4.0/>.

© The Author(s) 2025